

A consensus-based secondary control layer for stable current sharing and voltage balancing in DC microgrids

Michele Tucci^{*1}, Lexuan Meng^{†2}, Josep M. Guerrero^{‡ 2}, and Giancarlo Ferrari-Trecate^{§ 3}

¹*Dipartimento di Ingegneria Industriale e dell'Informazione, Università degli Studi di Pavia, Italy*

²*Institute of Energy Technology, Aalborg University, Denmark*

³*Automatic Control Laboratory, École Polytechnique Fédérale de Lausanne (EPFL), Switzerland*

Technical Report

March, 2016

Abstract

In this paper, we propose a secondary consensus-based control layer for current sharing and voltage balancing in DC microGrids (mGs). To this purpose, we assume that Distributed Generation Units (DGUs) are equipped with decentralized primary controllers guaranteeing voltage stability. This goal can be achieved using, for instance, Plug-and-Play (PnP) regulators. We analyze the behavior of the closed-loop mG by approximating local primary control loops with either unitary gains or first-order transfer functions. Besides proving exponential stability, current sharing, and voltage balancing, we describe how to design secondary controllers in a PnP fashion when DGUs are added or removed. Theoretical results are complemented by simulations, using a 5-DGUs mG implemented in Simulink/PLECS, and experiments on a 3-DGUs mG.

^{*}Electronic address: michele.tucci02@universitadipavia.it

[†]Electronic address: menglexuan@gmail.com; Corresponding author

[‡]Electronic address: joz@et.aau.dk

[§]Electronic address: giancarlo.ferrari@epfl.ch

1 Introduction

Power generation and distribution are rapidly changing due to the increasing diffusion of renewable energy sources, advances in energy storage, and active participation of consumers to the energy market [1]. This shift of paradigm has motivated the development of microGrids (mGs), commonly recognized as small-scale power systems integrating Distributed Generation Units (DGUs), storage devices and loads. Since AC power generation is the standard for commercial, residential, and industrial utilization, several studies focused on the control of AC mGs [2, 3, 4, 5, 6]. However, nowadays, DC energy systems are gaining interest [7, 8] because of the increasing number of DC loads, the availability of efficient converters, and the need of interfacing DC energy sources and batteries with minimal power losses. As reviewed in [8], DC mGs are becoming more and more popular in several application domains, such as avionics, automotive, marine and residential systems [8].

The basic problems in control of DC mGs are voltage stabilization [7, 9, 10, 11, 12, 13, 14] and current sharing (or, equivalently, load sharing), the latter meaning that DGUs must compensate constant load currents proportionally to given parameters (for example, the converter ratings) and independently of the mG topology and line impedances. Current sharing is crucial for preserving the safety of the system, as unregulated currents may overload generators and eventually lead to failures or system blackout [15]. An additional desirable goal is voltage balancing, i.e. to keep the average output voltage of DGUs close to a prescribed level. Indeed, load devices are designed to be supplied by a nominal reference voltage: it is therefore important to ensure that the voltages at the load buses are spread around this value.

These objectives can be realized using hierarchical control structures. In several works, current sharing regulation is realized in the primary layer, through decentralized droop controllers. However, droop regulators alone might fail to guarantee voltage stability. For solving this problem, in [16, 10, 17, 18, 19] it has been proposed to complement them with a secondary distributed control layer based on consensus algorithm. The main drawback of these approaches is that voltage stability critically depends on the communication network required by consensus protocols, and it can be compromised by communication faults, delays or cyber attacks. Another issue is that, in terms of control design, the tuning of stabilizing droop and consensus controllers is often done in a centralized fashion, i.e. exploiting knowledge about all DGUs and lines [7, 19]. Synthesis algorithms of this kind become prohibitive for large mGs. Moreover, they are unsuitable for mGs with flexible structure because, to preserve voltage stability, the plugging-in or -out of DGUs might require to update all local controllers in the mG. This motivated the development of *scalable* design procedures for local controllers as in [9, 20] and [10]. In [9] and [20], the aim is to stabilize the voltage only via primary decentralized controllers. These regulators, termed Plug-and-Play (PnP) have the following features: (i) the computation of a local controller for a DGU can be cast into a local optimization problem, (ii) each optimization problem exploits information about the DGU only [20] or, at most, the power lines connected to it [9], and (iii) when a DGU is plugged-in, no other DGUs [20], or at most neighboring DGUs [9], must update their local controllers.

The goal of this paper is to develop secondary regulators for achieving current sharing and voltage balancing, to be used on top of a primary stabilizing control layer. Similarly to [10], we exploit consensus filters requiring DGUs to communicate in real-time over a network with arbitrary, yet connected, topology. There are, however, two main differences between [10] and the present paper. First, as recalled above, in [10] the networked secondary layer is necessary for voltage stability, as primary loops induce steady-state voltage drifts. In our case, secondary controllers can be turned off without compromising voltage stability. Second, in [10] DGUs under the action of primary controllers are abstracted into ideal voltage regulators. We also use this simplification, but only for tutorial reasons and for developing basic mathematical tools that will allow us to extend the main results to the more realistic case where primary control loops are approximated with first-order transfer functions.

At the mathematical level, in order to prove current sharing and voltage balancing, we characterize the eigenstructure of the product of three matrices (\mathbb{LDM}), where \mathbb{L} and \mathbb{M} are the graph Laplacians associated to the electrical and the communication graphs, respectively, and D is a

diagonal positive definite matrix defining the desired ratios between balanced currents. While several studies focused on the properties of the product of stochastic matrices (see e.g. [21]), which are central in discrete-time consensus, to our knowledge products of Laplacians received much less attention.

The paper is organized as follows. Section 2 summarizes the electrical model of DGUs and PnP controllers. The secondary control layer is developed and analyzed in Sections 3 and 4. In particular, Section 4.4 shows that, similarly to the regulators in [9] and [20], secondary controllers can be designed in a PnP fashion. Section 5.1 demonstrates current sharing and voltage balancing through simulations in Simulink/PLECS [22], where non-idealities of real converters and lines have been taken into account. Finally, in Section 5.2 we present experimental tests performed on a real DC mG.

A preliminary version of the paper will be presented at the 20th IFAC World Congress. Differently from the conference version, the present paper includes (i) the proofs of Propositions 2-5 and Theorem 1, (ii) the more realistic case where primary control loops are approximated with first-order transfer functions, and (iii) experimental results and more detailed simulations.

Notation and basic definitions. The cardinality of the finite set S will be denoted with $|S|$. A weighted directed graph (*digraph*) $\mathcal{G} = (\mathcal{V}, \mathcal{E}, W)$ is defined by the set of nodes $\mathcal{V} = \{1, \dots, n\}$, the set of edges $\mathcal{E} \subseteq \mathcal{V} \times \mathcal{V}$ and the diagonal matrix $W \in \mathbb{R}^{|\mathcal{E}| \times |\mathcal{E}|}$ with $W_{ii} = w_i$, where $w_i \in \mathbb{R}$ is the weight associated to the edge $e_i \in \mathcal{E}$. The set of neighbors of node $i \in \mathcal{V}$ is $\mathcal{N}_i = \{j : (i, j) \in \mathcal{E} \text{ or } (j, i) \in \mathcal{E}\}$. A digraph \mathcal{G} is *weakly connected* if its undirected version is connected [23]. $Q(\mathcal{G}) \in \mathbb{R}^{|\mathcal{V}| \times |\mathcal{E}|}$ is the incidence matrix of \mathcal{G} [24]. The Laplacian matrix of \mathcal{G} is $\mathcal{L}(\mathcal{G}) = Q(\mathcal{G})WQ(\mathcal{G})^T$, and it is independent of the orientation of edges. The average of a vector $v \in \mathbb{R}^n$ is $\langle v \rangle = \frac{1}{n} \sum_{i=1}^n v_i$. We denote with H^1 the subspace composed by all vectors with zero average [25, 26] i.e. $H^1 = \{v \in \mathbb{R}^n : \langle v \rangle = 0\}$. The space orthogonal to H^1 is H_\perp^1 . It holds $H_\perp^1 = \{\alpha \mathbf{1}_n, \alpha \in \mathbb{R}\}$ and $\dim(H_\perp^1) = 1$. Moreover, the decomposition $\mathbb{R}^n = H^1 \oplus H_\perp^1$ is direct, i.e. each vector $v \in \mathbb{R}^n$ can always be written in a unique way as

$$v = \hat{v} + \bar{v} \quad \text{with } \hat{v} \in H^1 \text{ and } \bar{v} \in H_\perp^1. \quad (1)$$

Consider the matrix $A \in \mathbb{R}^{n \times n}$. With $A(H^1|H^1)$ we indicate the linear map $A : H^1 \rightarrow H^1$ (i.e. the restriction of the map $A : \mathbb{R}^n \rightarrow \mathbb{R}^n$ to the subspace H^1). For a subspace $\mathcal{V} \subset \mathbb{R}^n$, we denote with $P_{\mathcal{V}}(v)$ the projection of $v \in \mathbb{R}^n$ on \mathcal{V} . The subspace $\mathcal{V} \subset \mathbb{R}^n$ is said to be *A-invariant* if $v \in \mathcal{V} \Rightarrow Av \in \mathcal{V}$.

Let $A \in \mathbb{R}^{n \times n}$ be a matrix with real eigenvalues. The *inertia* of A is the triple

$$i(A) = (i_+(A), i_-(A), i_0(A)),$$

where $i_+(A)$ is the number of positive eigenvalues of A , $i_-(A)$ is the number of negative eigenvalues of A , and $i_0(A)$ is the number of zero eigenvalues of A , all counted with their algebraic multiplicity [27].

Laplacian matrices have the key properties summarized in the next Proposition [28, 29, 25].

Proposition 1. *For a weakly connected graph \mathcal{G} with weights $w_i > 0$, $A = \mathcal{L}(\mathcal{G}) \in \mathbb{R}^{n \times n}$ has the following properties:*

- (i) *it has non positive off-diagonal elements;*
- (ii) $\lambda_1(A) \geq \dots \geq \lambda_{n-1}(A) \geq 0 = \lambda_n$;
- (iii) $\text{Ker}(A) = H_\perp^1$ and $\text{Range}(A) = H^1$;
- (iv) $A(H^1|H^1)$ *is invertible.*

Proof. Points (i)-(iii) are shown, e.g. in [28, 29]. Point (iv) has been shown in [25] with the framework of partial difference equations. Next, we provide a proof based on linear algebra only. We start noticing that the linear map $A(H^1|H^1)$ invertible if it is surjective and injective [30]. First, we show the surjectivity of A on H^1 . By construction, $\text{rank}(A) = n - 1$ because

$$\text{rank}(A) = \dim(\text{Range}(A)) = \dim(\mathbb{R}^n) - \dim(H_\perp^1) = n - 1.$$

Moreover, since A is symmetric, each column of A has zero sum and hence is a vector in H^1 . Since $\text{Range}(A)$ is the column span, then $\text{Range}(A) \subseteq H^1$. Since $\dim(H^1) = n - 1$, one obtains $\text{Range}(A) = H^1$. This proves that the map $A(H^1|H^1)$ is surjective.

Next, we prove that $A(H^1|H^1)$ is also injective. By definition, this holds if

$$\forall b \in H^1 \quad \forall x, y \in H^1 \quad (Ax = b \text{ and } Ay = b) \Rightarrow x = y.$$

Now, $Ax = Ay = b$ implies that $A(x - y) = 0$. It means that $x - y \in \text{Ker}(A)$, therefore $\exists \alpha \in \mathbb{R}$ such that $x - y = \alpha \mathbf{1}_n$. However, since $x - y \in H^1$, $x - y = \alpha \mathbf{1}_n$ is verified only for $\alpha = 0$; this leads to $x = y$. \square

2 Plug-and-play primary voltage control

2.1 DGU electrical model

As in [9], we consider a DC mG composed of N DGUs, whose electrical scheme is shown in Figure 1. In each DGU, the generic renewable resource is modeled as a battery and a Buck converter is used to supply a local load connected to the Point of Common Coupling (PCC) through an RLC filter. Furthermore, we assume that loads I_{Li} are unknown and treated as current disturbances [9, 20]. The controlled variable is the voltage at each PCC. From Figure 1, by applying Kirchoff's voltage and current laws and exploiting Quasi Stationary Line (QSL) approximation of power lines [9, 20], we obtain the following model of DGU i ¹

$$\text{DGU } i : \begin{cases} \frac{dV_i}{dt} = \frac{1}{C_{ti}} I_{ti} + \sum_{j \in \mathcal{N}_i} \left(\frac{V_j}{C_{ti} R_{ij}} - \frac{V_i}{C_{ti} R_{ij}} \right) - \frac{1}{C_{ti}} I_{Li} \\ \frac{dI_{ti}}{dt} = -\frac{1}{L_{ti}} V_i - \frac{R_{ti}}{L_{ti}} I_{ti} + \frac{1}{L_{ti}} V_{ti} \end{cases}$$

where inputs (V_{ti}, I_{Li}) and $V_j \in \mathcal{N}_i$, states (V_i, I_{ti}) , and electrical parameters R_{ti}, C_{ti}, L_{ti} and R_{ij} are shown in Figure 1. In particular, V_i and I_{ti} are the measured voltage at the i -th PCC and i -th output current, respectively, while V_j is the voltage at the PCC of each neighboring DGU $j \in \mathcal{N}_i$.

2.2 Plug-and-play regulators

In this Section, we briefly summarize the PnP scalable approach in [9, 20] for designing primary decentralized controllers guaranteeing voltage stability in DC mGs. This will allow us to justify the approximations of primary control loops used in Section 4. Moreover, we will describe local updates that must be performed when DGUs are added or removed. Similar operations will be described in Section 4.4 for updating local secondary controllers, hence showing that both the primary and secondary control layer can be designed in a modular and scalable fashion.

The local regulator of DGU i exploits measurements of V_i and I_{ti} to compute the command V_{ti} of the i -th Buck converter and make V_i track a reference signal $V_{ref,i}$ (see the scheme in Figure 1). Each controller is composed of a vector gain K_i and an integral action is present for offset-free voltage tracking. The decentralized computation of these vector gains is the core of PnP controller synthesis: (i) the design of K_i requires knowledge of the dynamics of DGU i only [20] or, at most, the parameters of power lines connecting it to its neighbors [9], (ii) K_i is automatically obtained by solving a Linear Matrix Inequality (LMI) problem.

For modeling the interaction of multiple DGUs, we represent the mG with a digraph $\mathcal{G}_{el} = (\mathcal{V}_{el}, \mathcal{E}_{el}, W)$ (see the example in Figure 2), where (i) each node is a DGU with local PnP controller and local current load, (ii) edges (i, j) are power lines whose orientation define a reference direction for positive currents, (iii) weights are line conductances² $\frac{1}{R_{ij}}$, and (iv) we set $N = |\mathcal{V}_{el}|$ and $M = |\mathcal{E}_{el}|$.

¹For the detailed model derivation, we defer the reader to [9].

²Line inductances L_{ij} are neglected as we assume QSL approximations [9, 20].

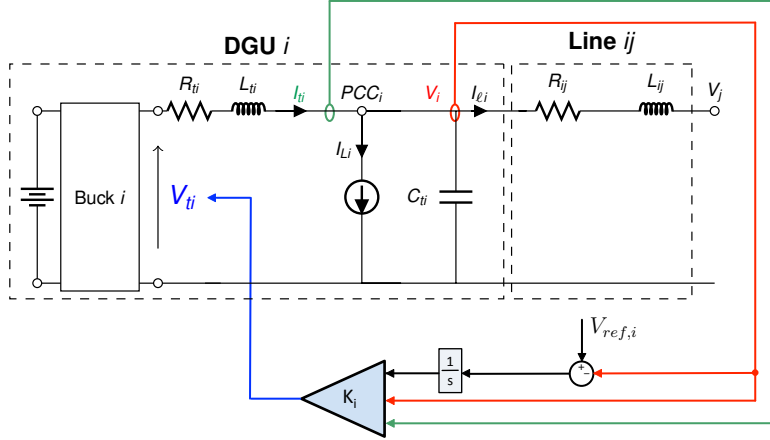


Figure 1: Electrical scheme of DGU i and local PnP voltage controller.

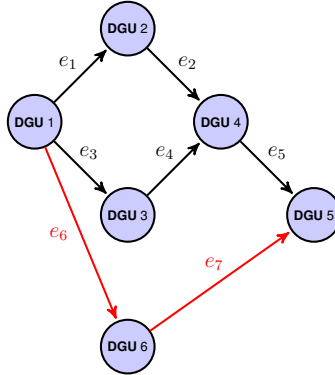


Figure 2: Graph representation of an mG composed of 5 DGUs (in black) and plug-in of DGU 6 (in red).

Next, we describe how to handle plugging -in/-out of DGUs while preserving the stability of the mG. Whenever a DGU (say DGU i) wants to join the network (e.g. DGU 6 in Figure 2), it sends a plug-in request to its future neighbors, i.e. DGUs $j \in \mathcal{N}_i$ (e.g. DGUs 1 and 5 in Figure 2). Then, DGU i [20] or each DGU in the set $\{i\} \cup \mathcal{N}_i$ [9] solves an LMI problem ((24) in [20] and (25) in [9]) that, if feasible, gives a vector gain K_i guaranteeing voltage stability in the whole mG after the addition of DGU i . Otherwise, if one of the LMIs is infeasible, the plug-in of DGU i is denied and no update of matrices K_j , $j \in \mathcal{N}_i$ is performed.

The unplugging of a DGU (say DGU m) follows a similar procedure. It is always allowed without redesigning any local controller [20] or it requires to successfully update, at most, controllers of DGUs k , $k \in \mathcal{N}_m$ before allowing the disconnection of the DGU [9].

Remark 1. *Local PnP controllers can be enhanced with pre-filters so as to shape in a desired way the transfer function $F_{[i]}(s)$ between voltages $V_{ref,i}$ and V_i represented in Figure 1. The closed-loop transfer function $F_{[i]}(s)$ has 3 poles and in the sequel it will be approximated by an unit gain or a first-order system. The first approximation will be used mainly for tutorial reasons. The second one is very mild at low and medium frequencies, as it can be noticed from the Bode plots of $F_{[i]}(s)$ in [9]. Moreover, the presence of an integrator in Figure 1 allows the voltage V_i at the PCC to track constant references without offset when the disturbances (i.e. load currents I_{Li}) are constant.*

3 Secondary control based on consensus algorithms

Primary stabilizing controllers, such as the PnP regulators described in Section 2.2, have the goal of turning DGUs into controlled voltage generators, i.e. to approximate, as well as possible, the identity $V_i = V_{ref,i}$. As such, they do not ensure current sharing and voltage balancing, defined in the sequel.

Definition 1. For constant load currents $I_{Li}, i = 1, \dots, N$, current sharing is achieved if, at steady state, the overall load current is proportionally shared among DGUs, i.e. if

$$\frac{I_{ti}}{I_{ti}^s} = \frac{I_{tj}}{I_{tj}^s} \quad \text{for all } i, j \in \mathcal{V}_{el}, \quad (2)$$

where $I_{ti}^s > 0$ are scaling factors.

We recall that current sharing is desirable in order to avoid situations in which some DGUs are not able to supply local loads, thus requiring power from other DGUs. A very common goal is to make DGUs share the total load current proportionally to their generation capacity. This can be obtained by measuring the output currents in per-unit (p.u.), i.e. setting each scaling factor I_{ti}^s in (2) equal to the corresponding DGU rated current (see Section 5.1 for an example). On the other hand, if the scaling factors are all identical, the current sharing condition becomes

$$I_{ti} = \langle \mathbf{I}_L \rangle \quad i = 1, \dots, N, \quad (3)$$

where $\mathbf{I}_L = [I_{L1}, I_{L2}, \dots, I_{LN}]^T$ is the vector of the local load currents.

Assumption 1. Voltage references are identical for all DGUs, i.e. $V_{ref,i} = V_{ref}, \forall i \in \mathcal{V}_{el}$.

Definition 2. Under Assumption 1, voltage balancing is achieved if

$$\langle \mathbf{V} \rangle = V_{ref}. \quad (4)$$

where vector $\mathbf{V} = [V_1, V_2, \dots, V_N]^T$ collects the PCC voltages.

In order to guarantee current sharing and voltage balancing, we use a consensus-based secondary control layer. Consensus filters are commonly employed for achieving global information sharing or coordination through distributed computations [31, 23]. In our case, as shown in Figure 3, we adopt the following consensus scheme for adjusting the references of each primary voltage regulator

$$\dot{\Delta V}_i(t) = k_I \sum_{j=1, j \neq i}^N a_{ij} \left(\frac{I_{ti}(t)}{I_{ti}^s} - \frac{I_{tj}(t)}{I_{tj}^s} \right), \quad (5)$$

where $a_{ij} > 0$ if DGUs i and j are connected by a communication link ($a_{ij} = 0$, otherwise), and the coefficient $k_I > 0$ is common to all DGUs. The use of consensus protocols has been thoroughly studied for networks of agents with simple dynamics, e.g. simple integrators [31, 23], with the goal of proving convergence of individual states to a common value. In our case, however, (5) is interfaced with the mG dynamics and convergence of currents I_{ti} to the same value does not trivially follow from standard consensus theory. This property will be rigorously analyzed in Section 4.

In the sequel, we assume bidirectional communication, i.e. $a_{ij} = a_{ji}$. The corresponding communication digraph is $\mathcal{G}_c = (\mathcal{V}_{el}, \mathcal{E}_c, W_c)$ where $(i, j) \in \mathcal{E}_c \iff a_{ij} > 0$ and $W_c = \text{diag}\{a_{ij}\}$. Note that the topology of \mathcal{G}_c and \mathcal{G}_{el} can be completely different. From now on, we will make the following standing assumption.

Assumption 2. The graphs \mathcal{G}_{el} and \mathcal{G}_c are weakly connected.

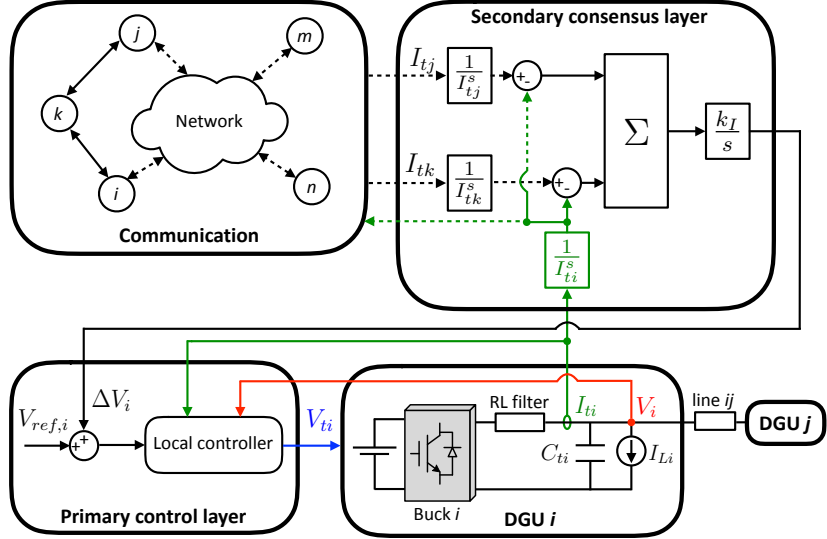


Figure 3: Complete hierarchical control scheme of DGU i .

From a system point of view, the collective dynamics of the group of DGUs following (5) can be expressed as

$$\dot{\Delta \mathbf{V}} = - \underbrace{k_I L D \mathbf{I}_t}_{\mathbb{L}}, \quad (6)$$

where $\Delta \mathbf{V} = [\Delta V_1, \dots, \Delta V_N]^T = \mathbf{V} - \mathbf{V}_{\text{ref}}$, $\mathbf{V}_{\text{ref}} = [V_{\text{ref},1}, V_{\text{ref},2}, \dots, V_{\text{ref},N}]^T$, $\mathbf{I}_t = [I_{t1}, I_{t2}, \dots, I_{tN}]^T$, $D = \text{diag}\left(\frac{1}{I_{t1}^s}, \dots, \frac{1}{I_{tN}^s}\right) = \text{diag}(d_1, \dots, d_N)$ and $L = \mathcal{L}(\mathcal{G}_c)$. Note that \mathbb{L} is the Laplacian matrix of \mathcal{G}_c with W_c replaced by $k_I W_c$.

4 Modeling and analysis of the complete system

The hierarchical control scheme of a DGU equipped with primary and secondary regulators is shown in Figure 3. For studying the behavior of the closed-loop mG, we first approximate DGUs under the effect of primary controllers by unit gains (Section 4.1) and prove that current sharing is achieved in a stable way. We also provide conditions for voltage balancing. Results derived in this simple setting will be instrumental for studying the more complex scheme where primary control loops are abstracted into first-order transfer functions (Section 4.3).

4.1 Unit-gain approximation of primary control loops

By approximating primary loops with ideal unit gains, we have the relations $V_i = V_{\text{ref},i} + \Delta V_i$, $\forall i \in \mathcal{V}_{\text{el}}$.

Figures 4a-4b show the resulting control scheme, used for deriving the dynamics of the overall mG as a function of the inputs \mathbf{I}_L and \mathbf{V}_{ref} . Starting from the left-hand side of Figure 4a, we have, in order, (6) and

$$\mathbf{V} = \Delta \mathbf{V} + \mathbf{V}_{\text{ref}}. \quad (7)$$

Then, from basic circuit theory, we derive the relation between the vector of voltages \mathbf{V} and the vector of line currents $\mathbf{I}_\ell = [I_{\ell 1}, \dots, I_{\ell M}]^T$ as

$$\mathbf{I}_\ell = -WB^T\mathbf{V}, \quad (8)$$

where W and $B = Q(\mathcal{G}_{\text{el}})$ are the weight and the incidence matrix of \mathcal{G}_{el} , respectively. Next, we get

$$\mathbf{I}_t = \mathbf{I}_L - BI_\ell \quad (9)$$

and, merging equations (6)-(9), we finally obtain

$$\begin{aligned}\Sigma : \dot{\Delta \mathbf{V}} &= -\mathbb{L}D \underbrace{BWB^T}_{\mathbb{M}} \Delta \mathbf{V} - \mathbb{L}D \mathbf{I}_L - \mathbb{L}D \underbrace{BWB^T}_{\mathbb{M}} \mathbf{V}_{\text{ref}} \\ &= -\mathbb{Q} \Delta \mathbf{V} - \mathbb{L}D \mathbf{I}_L - \mathbb{Q} \mathbf{V}_{\text{ref}}\end{aligned}\quad (10)$$

where $\mathbb{M} = \mathcal{L}(\mathcal{G}_{el}) = BWB^T$ is the Laplacian matrix of the electrical network and $\mathbb{Q} = \mathbb{L}DM$.

4.2 Properties of the matrix \mathbb{Q}

The matrix \mathbb{Q} in (10) captures the interaction of electric couplings and communication. From (10), it governs the voltage dynamics and hence the achievement of current sharing and voltage balancing. Notice that \mathbb{Q} is obtained pre- and post- multiplying a diagonal matrix by a Laplacian (\mathbb{L} and \mathbb{M} , respectively). It follows that \mathbb{Q} is not a Laplacian matrix itself because it might fail to be symmetric and have positive off-diagonal entries, even if weights of \mathcal{G}_{el} and \mathcal{G}_c are positive. Nevertheless, in the sequel, we demonstrate that \mathbb{Q} preserves some key features of Laplacian matrices. Before showing this, we introduce a preliminary result.

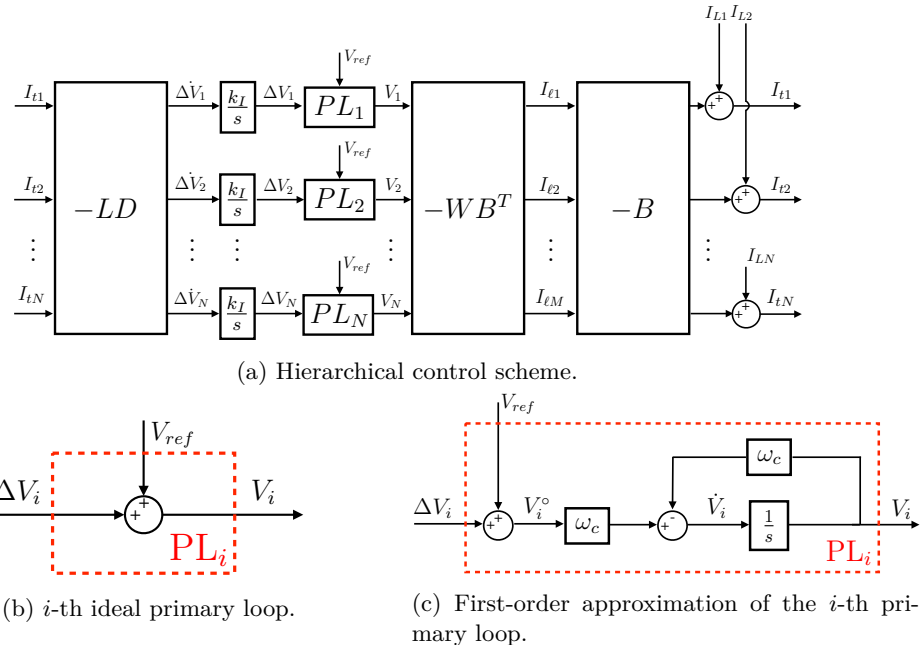


Figure 4: Hierarchical control scheme and Primary Loop (PL) approximations.

Proposition 2. *It holds $P_{H^1}(DMH^1) = H^1$.*

Proof. From Proposition 1-(iv), we know that $\mathbb{M}(H^1|H^1)$ is invertible, hence surjective. Then,

$$DMH^1 = DH^1.$$

We now study the projection map $P_{H^1} : DH^1 \rightarrow H^1$. Since D is invertible, we have that $\dim(DH^1) = \dim(H^1) = N - 1$. Therefore, one has

$$\dim(\text{Range}(P_{H^1})) + \dim(\text{Ker}(P_{H^1})) = N - 1. \quad (11)$$

The next step is to show that

$$\text{Ker}(P_{H^1}) = \{0\}, \quad (12)$$

so that, from (11), P_{H^1} is surjective. Let $u \in DH^1$ and set $u = \bar{u} + \hat{u}$, where $\bar{u} \in H_\perp^1$ and $\hat{u} \in H^1$. Hence, $P_{H^1}u = P_{H^1}\hat{u} = \hat{u}$ and, if $u \in \text{Ker}(P_{H^1})$, then $\hat{u} = 0$. In other words, $u \in \text{Ker}(P_{H^1})$ verifies

$$\begin{cases} u = \alpha_u \mathbf{1} & \text{for some } \alpha_u \in \mathbb{R} \\ u = Dv & \text{for some } v \in H^1 \end{cases}$$

One has

$$\|u\|_{D^{-1}}^2 = u^T D^{-1} u = \alpha_u \mathbf{1}^T D^{-1} D v = \alpha_u \mathbf{1}^T v = 0$$

where the last identity follows from the fact that $v \in H^1$ has zero average. But, since $\|\cdot\|_{D^{-1}}$ is a norm, $\|u\|_{D^{-1}}^2$ implies $u = 0$. This shows (12). \square

Proposition 3. *The matrix $\mathbb{Q} = \mathbb{LDM}$ has the following properties:*

- (i) $\text{Ker}(\mathbb{Q}) = H_\perp^1$;
- (ii) $\text{Range}(\mathbb{Q}) = H^1$;
- (iii) the linear transformation $\mathbb{Q}(H^1|H^1)$ is invertible;
- (iv) \mathbb{Q} has real nonnegative eigenvalues;
- (v) the zero eigenvalue of \mathbb{Q} has algebraic multiplicity equal to one.

Proof. We start by proving point (ii). Since, from Proposition 1-(iii), $\text{Ker}(\mathbb{M}) = H_\perp^1$, one has $\mathbb{M}\mathbb{R}^N = \mathbb{M}(H_\perp^1 \oplus H^1) = \mathbb{M}H^1$. Furthermore, from Proposition 2, $P_{H^1}(\mathbb{D}\mathbb{M}H^1) = H^1$. Proposition 1-(iv) applied to the Laplacian \mathbb{L} shows that $\mathbb{L}(\mathbb{D}\mathbb{M}\mathbb{R}^N) = H^1$, which is (ii).

For proving point (i), we recall that $\text{Ker}(\mathbb{M}) = H_\perp^1$ and then $\text{Ker}(\mathbb{LDM}) \supseteq H_\perp^1$. From (ii) we have that $\dim(\text{Range}(\mathbb{Q})) = N - 1$. The equation $\dim(\text{Range}(\mathbb{Q})) + \dim(\text{Ker}(\mathbb{Q})) = N$ implies that $\dim(\text{Ker}(\mathbb{Q})) = 1$. Since $\dim(H_\perp^1) = 1$, we have $\text{Ker}(\mathbb{Q}) = H_\perp^1$.

In order to prove point (iii), we show that $\mathbb{Q}(H^1|H^1)$ is both surjective and injective. The surjectivity of \mathbb{Q} on H^1 has been shown above when proving point (ii). For proving the injectivity, we need to check if it holds

$$\forall b \in H^1 \quad \forall x, y \in H^1 \quad (\mathbb{Q}x = b \text{ and } \mathbb{Q}y = b) \Rightarrow x = y.$$

Now, $\mathbb{Q}x = \mathbb{Q}y = b$ implies that $\mathbb{Q}(x - y) = 0$. It means that $x - y \in \text{Ker}(\mathbb{Q}) = H_\perp^1$, therefore $\exists \alpha \in \mathbb{R}$ such that $x - y = \alpha \mathbf{1}_n$. However, since $x - y \in H^1$, $x - y = \alpha \mathbf{1}_n$ is verified only for $\alpha = 0$; this leads to $x = y$.

As regards statement (iv), note that D is diagonal with positive elements. Therefore, \mathbb{Q} can be written as follows

$$\mathbb{Q} = D^{-\frac{1}{2}} \underbrace{D^{\frac{1}{2}} \mathbb{L} D^{\frac{1}{2}}}_{\mathcal{L}} \underbrace{D^{\frac{1}{2}} \mathbb{M} D^{\frac{1}{2}}}_{\mathcal{M}} D^{-\frac{1}{2}}. \quad (13)$$

By construction, matrices \mathcal{L} and \mathcal{M} in (13) are positive semidefinite in the real sense. Moreover, they are symmetric, hence they are positive semidefinite also in the complex sense [32]. Therefore, we can apply Corollary 2.3 in [27], which states that the product of two complex positive semidefinite matrices is diagonalizable and has nonnegative real eigenvalues. Moreover, since $D^{-\frac{1}{2}}$ in (13) is symmetric, matrix $\mathcal{L}\mathcal{M}$ is congruent to \mathbb{Q} . Thus, by Sylvester's law of inertia [33], the inertia of \mathbb{Q} and $\mathcal{L}\mathcal{M}$ coincide, i.e.

$$(i_+(\mathcal{L}\mathcal{M}), 0, i_0(\mathcal{L}\mathcal{M})) = (i_+(\mathbb{Q}), 0, i_0(\mathbb{Q})). \quad (14)$$

This proves (iv).

Finally, in order to prove (v), we first show that $\dim(\text{Ker}(\mathcal{L}\mathcal{M})) = 1$, which allows us to say that the algebraic multiplicity of the zero eigenvalue of $\mathcal{L}\mathcal{M}$ is equal to one (because $\mathcal{L}\mathcal{M}$ is diagonalizable). Then, we exploit $i_0(\mathcal{L}\mathcal{M}) = i_0(\mathbb{Q})$ in (14) to conclude. We show that, since D is nonsingular, in view of (13)

$$\dim(\text{Ker}(\mathcal{L}\mathcal{M})) = \dim(\text{Ker}(\mathbb{Q})) = 1, \quad (15)$$

where the last equality follows from point (i). From (13) and point (i), we have that

$$D^{-\frac{1}{2}}H_{\perp}^1 \subseteq \text{Ker}(D^{-\frac{1}{2}}\mathcal{LM}) = \text{Ker}(\mathcal{LM}), \quad (16)$$

where the last identity follows from $\det(D^{-\frac{1}{2}}) \neq 0$. Assume, by contradiction, that the inclusion is strict. Then, there is $x \in \mathbb{R}^N$, $x \neq 0$, such that

$$\mathcal{LM}x = 0 \quad (17a)$$

$$x \neq \alpha \mathbf{d} \quad \forall \alpha \in \mathbb{R}, \quad (17b)$$

where $\mathbf{d} = [d_1^{-\frac{1}{2}}, \dots, d_N^{-\frac{1}{2}}]^T$. From (17a), one has that $D^{-\frac{1}{2}}\mathcal{LM}x = 0$. Setting $v = D^{\frac{1}{2}}x$, it also holds $D^{-\frac{1}{2}}\mathcal{LM}D^{-\frac{1}{2}}v = 0$, that is $\mathbb{Q}v = 0$. From point (i), $v \in H_{\perp}^1$ and therefore $x = \alpha \mathbf{d}$, for some $\alpha \neq 0$. This contradicts (17b). \square

4.2.1 Analysis of equilibria

In order to evaluate the steady-state behavior of the electrical signals appearing in Figure 4a-4b, we study the equilibria of system (10). Hence, for given constant inputs $(\mathbf{I}_L^*, \mathbf{V}_{\text{ref}}^*)$, we characterize the solutions $\Delta \mathbf{V}^*$ of equation

$$\mathbb{Q}\Delta \mathbf{V}^* = -\mathbb{L}D\mathbf{I}_L^* - \mathbb{Q}\mathbf{V}_{\text{ref}}^* \quad (18)$$

through the following Proposition.

Proposition 4. *For equation (18),*

(i) *there is only one solution $\widetilde{\Delta \mathbf{V}}^* \in H^1$;*

(ii) *all solutions $\Delta \mathbf{V}^* \in \mathbb{R}^N$ can be written as*

$$\Delta \mathbf{V}^* = \widetilde{\Delta \mathbf{V}}^* + \alpha \mathbf{1}_N \quad \alpha \in \mathbb{R}. \quad (19)$$

Proof. Proposition 3-(ii) shows that (18) has solutions only if $-\mathbb{L}D\mathbf{I}_L^* - \mathbb{Q}\mathbf{V}_{\text{ref}}^* \in H^1$. From Propositions 1-(iii) and 3-(ii) this is always true. Statement (i) directly follows from Proposition 3-(iii).

For the proof of statement (ii), we split $\Delta \mathbf{V}^* \in \mathbb{R}^N$ as in (1), i.e. $\Delta \mathbf{V}^* = \widehat{\Delta \mathbf{V}}^* + \overline{\Delta \mathbf{V}}^*$. From (18) and Proposition 3-(i), one has that, irrespectively of $\widehat{\Delta \mathbf{V}}^* = \alpha \mathbf{1}_N \in H_{\perp}^1$, $\mathbb{Q}\widehat{\Delta \mathbf{V}}^* = -\mathbb{L}D\mathbf{I}_L^* - \mathbb{Q}\mathbf{V}_{\text{ref}}^*$. Moreover, from the first part of the proof, it holds $\widehat{\Delta \mathbf{V}}^* = \widetilde{\Delta \mathbf{V}}^*$. \square

Next, we relate properties of the equilibria of (10) to current sharing and voltage balancing.

Proposition 5. *Consider system (10) with constant inputs $(\mathbf{I}_L^*, \mathbf{V}_{\text{ref}}^*)$. Then, current sharing is achieved at steady state. Moreover, if $\mathbf{V}_{\text{ref}}^* = V_{\text{ref}} \mathbf{1}_N$ (i.e. if Assumption 1 holds) and α in (19) is equal to zero, then the equilibrium \mathbf{V}^* verifies the voltage balancing condition (4).*

Proof. At the equilibrium, since $\text{Ker}(\mathbb{L}) = H_{\perp}^1$ (see Proposition 1-(iii)), from (6) we have that

$$\begin{aligned} -\mathbb{L}D\mathbf{I}_t^* = \mathbf{0}_N &\Leftrightarrow D\mathbf{I}_t^* = \bar{I}_t \mathbf{1}_N \\ &\Leftrightarrow \left[\frac{I_{t1}^*}{I_{t1}^s}, \dots, \frac{I_{tN}^*}{I_{tN}^s} \right]^T = \bar{I}_t \mathbf{1}_N, \end{aligned} \quad (20)$$

which is (2). Let now $\Delta \mathbf{V}^*$ be an equilibrium for system (10). Replacing (19) in (7) and averaging the resulting vector, we get

$$\langle \mathbf{V}^* \rangle = \underbrace{\langle \widetilde{\Delta \mathbf{V}}^* \rangle}_{=0} + \underbrace{N\alpha}_{=0} + V_{\text{ref}},$$

which is (4). \square

4.2.2 Stability analysis

The similarities established in Proposition 3 between the spectral properties of graph Laplacians and the matrix \mathbb{Q} , will allow us to study the stability properties of (10) pretty much as it is done in the analysis of classical consensus dynamics. Results in this Section follow the approach in [26], where exponentially stable consensus is analyzed through the use of invariant subspaces. An advantage of this rationale is that it carries over almost invariably to the case of more complex models of primary loops (Section 4.3).

In the sequel, we prove exponentially stable convergence of $\Delta\mathbf{V}$ in (10) to an equilibrium ensuring both current sharing and voltage balancing for constant \mathbf{I}_L^* and $\mathbf{V}_{ref}^* = V_{ref}\mathbf{1}_N$. We first show that projections $P_{H_\perp^1}(\Delta\mathbf{V}) = \overline{\Delta\mathbf{V}}$ and $P_{H^1}(\Delta\mathbf{V}) = \widehat{\Delta\mathbf{V}}$ have non-interacting dynamics (or, equivalently, that subspaces H^1 and H_\perp^1 are invariant for (10)).

Proposition 6. *If $\Delta\mathbf{V}$ is given by system Σ in (10) for $\Delta\mathbf{V}(0) = \Delta\mathbf{V}_0$, then $\Delta\mathbf{V} = \overline{\Delta\mathbf{V}} + \widehat{\Delta\mathbf{V}}$, where $\overline{\Delta\mathbf{V}} \in H_\perp^1$ and $\widehat{\Delta\mathbf{V}} \in H^1$ fulfill*

$$\bar{\Sigma} : \begin{cases} \dot{\overline{\Delta\mathbf{V}}} = \mathbf{0}_N \\ \overline{\Delta\mathbf{V}}(0) = \langle \Delta\mathbf{V}_0 \rangle \mathbf{1}_N \end{cases} \quad (21)$$

and

$$\hat{\Sigma} : \begin{cases} \dot{\widehat{\Delta\mathbf{V}}} = -\mathbb{Q}\widehat{\Delta\mathbf{V}} - \mathbb{L}D\mathbf{I}_L - \mathbb{Q}\mathbf{V}_{ref} \\ \widehat{\Delta\mathbf{V}}(0) = \Delta\mathbf{V}_0 - \overline{\Delta\mathbf{V}}_0. \end{cases} \quad (22)$$

Proof. We write vectors $\Delta\mathbf{V}(0)$, \mathbf{I}_L and \mathbf{V}_{ref} according to the decomposition (1), i.e. using “ \wedge ” and “ $-$ ” for denoting their H^1 and H_\perp^1 components, respectively. As described in [26], we analyze the dynamics of $\overline{\Delta\mathbf{V}}$ by averaging both sides of (10) and $\Delta\mathbf{V}(0) = \Delta\mathbf{V}_0$, respectively. From points (i)-(ii) of Proposition 3, we have $\langle -\mathbb{Q}\Delta\mathbf{V} \rangle = 0$ and $\langle -\mathbb{Q}\mathbf{V}_{ref} \rangle = 0$. Since $\text{Range}(\mathbb{L}) = H^1$ (see Proposition 1-(iii)), we also have $\langle -\mathbb{L}D\mathbf{I}_L \rangle = 0$, hence obtaining $\frac{d}{dt}\langle \Delta\mathbf{V} \rangle = 0$. Recalling that $\overline{\Delta\mathbf{V}}_0 = \langle \Delta\mathbf{V}_0 \rangle \mathbf{1}_N$, we obtain (21).

Next, we analyze $\widehat{\Delta\mathbf{V}} = \Delta\mathbf{V} - \overline{\Delta\mathbf{V}}$. We have

$$\dot{\widehat{\Delta\mathbf{V}}} = \dot{\Delta\mathbf{V}} - \underbrace{\dot{\overline{\Delta\mathbf{V}}}}_{= \mathbf{0}_N} = -\mathbb{Q}\Delta\mathbf{V} - \mathbb{L}D\mathbf{I}_L - \mathbb{Q}\mathbf{V}_{ref}$$

and $\widehat{\Delta\mathbf{V}}(0) = \Delta\mathbf{V}_0 - \overline{\Delta\mathbf{V}}_0$. From Proposition 3-(i), $\mathbb{Q}\Delta\mathbf{V} = \mathbb{Q}\widehat{\Delta\mathbf{V}}$ and then we have (22). \square

Remark 2. *The splitting of Σ into systems $\bar{\Sigma}$ and $\hat{\Sigma}$ implies that, if $\Delta\mathbf{V}_0$ has zero average, then $\Delta\mathbf{V}(t)$ has the same property, $\forall t \geq 0$ and irrespectively of inputs $(\mathbf{I}_L, \mathbf{V}_{ref})$. This behavior can be realized by suitable initialization of the integrators appearing in Figure 4a.*

According to system $\bar{\Sigma}$, the value of $P_{H_\perp^1}(\Delta\mathbf{V}) = \overline{\Delta\mathbf{V}}$ remains constant over time and equal to $\overline{\Delta\mathbf{V}}_0$. Hence, in order to characterize the stability of equilibria (19), it is sufficient to study the dynamics (22). In an equivalent way, one can consider system (10) and the following definition of stability on a subspace.

Definition 3. *Let \mathcal{V} be a subspace of \mathbb{R}^n . The origin of $\dot{x} = \mathcal{A}x$, $x(t) \in \mathbb{R}^n$ is Globally Exponentially Stable (GES) on \mathcal{V} if $\exists \kappa, \eta > 0 : \|P_{\mathcal{V}}x(t)\| \leq \kappa e^{-\eta t} \|P_{\mathcal{V}}x(0)\|$. The parameter η is termed rate of convergence.*

Note that Σ is a linear system and, for stability analysis, we can neglect inputs, hence obtaining

$$\begin{cases} \dot{\Delta\mathbf{V}} = -\mathbb{Q}\Delta\mathbf{V} \\ \Delta\mathbf{V}(0) = \Delta\mathbf{V}_0. \end{cases} \quad (23)$$

Theorem 1. *The origin of (23) is GES on H^1 . Moreover, the rate of convergence is the smallest strictly positive eigenvalue of \mathbb{Q} .*

Proof. The proof of Theorem 1 is presented in Appendix A. \square

The above results reveal that, given an initial condition $\Delta\mathbf{V}(0) = \Delta\mathbf{V}_0$ for system (10) and constant inputs \mathbf{I}_L^* and $\mathbf{V}_{\text{ref}}^* = V_{\text{ref}}\mathbf{1}_N$, the state $\Delta\mathbf{V}$ converges to the equilibrium (19) with $\alpha = \langle \Delta\mathbf{V}_0 \rangle$.

Summarizing the main results of this Section, we have that the consensus scheme described by (5), Assumption 1 and

$$\langle \Delta\mathbf{V}_0 \rangle = 0 \quad (24)$$

guarantee the asymptotic achievement of current sharing and voltage balancing in a GES fashion. This happens independently of the weights k_I and a_{ij} in (5). Nevertheless, their precise value, as well as the topology of the communication graph, affect the rate of convergence.

4.3 First-order approximation of primary control loops

Figure 4a and Figure 4c show the overall closed-loop scheme of an mG equipped with (i) consensus current loops and (ii) primary control loops modeled as first-order transfer functions. Differently from the case analyzed in Section 4.1, each local dynamics is now described by means of two states which are the state of the consensus current loop (ΔV_i) and the state of the controlled DGU (V_i in Figure 4c). We highlight that relations (6) and (7) still hold, while the additional state equation is

$$\dot{\mathbf{V}} = \Omega\mathbf{V}^\circ - \Omega\mathbf{V}, \quad (25)$$

where vectors $\mathbf{V}^\circ = [V_1^\circ, V_2^\circ, \dots, V_N^\circ]^T$ and \mathbf{V} belong to \mathbb{R}^N , and the diagonal matrix $\Omega = \omega_c I \in \mathbb{R}^{N \times N}$, $\omega_c > 0$, collects on its diagonal the approximate bandwidth of each controlled DGU. In view of Remark 1, assuming equal approximate bandwidths for all the controlled DGUs is a mild constraint.

As in Section 4.1, in order to find the dynamics of the closed-loop scheme, we write relations among mG variables. From Figure 4a, we notice that (6) holds, and

$$\mathbf{V}^\circ = \Delta\mathbf{V} + \mathbf{V}_{\text{ref}}. \quad (26)$$

Always from Figure 4a, we have that, for line and output currents, equations (8) and (9) are still valid. By merging relations (6), (26), (25), (8) and (9), we can write the dynamics of the overall mG as

$$\begin{cases} \dot{\Delta\mathbf{V}} = -\mathbb{Q}\mathbf{V} - \mathbb{L}D\mathbf{I}_L \\ \dot{\mathbf{V}} = \Omega\Delta\mathbf{V} - \Omega\mathbf{V} + \Omega\mathbf{V}_{\text{ref}}, \end{cases} \quad (27a)$$

$$(27b)$$

or, equivalently, in compact form,

$$\begin{bmatrix} \dot{\Delta\mathbf{V}} \\ \dot{\mathbf{V}} \end{bmatrix} = \underbrace{\begin{bmatrix} \mathbf{0}_N & -\mathbb{Q} \\ \Omega & -\Omega \end{bmatrix}}_{\mathcal{Q}} \begin{bmatrix} \Delta\mathbf{V} \\ \mathbf{V} \end{bmatrix} + \begin{bmatrix} \mathbf{0}_N & -\mathbb{L}D \\ \Omega & -\Omega \end{bmatrix} \begin{bmatrix} \mathbf{V}_{\text{ref}} \\ \mathbf{I}_L \end{bmatrix},$$

with $\mathcal{Q} \in \mathbb{R}^{2N \times 2N}$ and $[\Delta\mathbf{V}^T \mathbf{V}^T]^T \in \mathbb{R}^N \times \mathbb{R}^N$.

4.3.1 Analysis of equilibria

The equilibria of system (27) for constant inputs $(\mathbf{I}_L^*, \mathbf{V}_{\text{ref}}^*)$, are obtained by computing the solutions $[\Delta\mathbf{V}^{*T}, \mathbf{V}^{*T}]^T$ to the system

$$\begin{cases} \mathbb{Q}\mathbf{V}^* = -\mathbb{L}D\mathbf{I}_L^* \\ \mathbf{0}_N = \Omega\Delta\mathbf{V}^* - \Omega\mathbf{V}^* + \Omega\mathbf{V}_{\text{ref}}^*. \end{cases} \quad (28a)$$

$$(28b)$$

Since matrix Ω is invertible, equation (28b) becomes

$$\mathbf{V}^* = \Delta \mathbf{V}^* + \mathbf{V}_{\text{ref}}^*. \quad (29)$$

By substituting (29) in (28a), we get

$$\mathbb{Q} \Delta \mathbf{V}^* = -\mathbb{L} D \mathbf{I}_L^* - \mathbb{Q} \mathbf{V}_{\text{ref}}^*.$$

that is exactly (18). We can then exploit Proposition 4 for concluding that there are infinitely many solutions $\Delta \mathbf{V}^* \in \mathbb{R}^N$ in the form (19). Replacing (19) in (29), we can write equilibria of system (27) as

$$\begin{bmatrix} \Delta \mathbf{V}^* \\ \mathbf{V}^* \end{bmatrix} = \begin{bmatrix} \widehat{\Delta \mathbf{V}}^* + \alpha \mathbf{1}_N \\ \widehat{\Delta \mathbf{V}}^* + \alpha \mathbf{1}_N + \mathbf{V}_{\text{ref}}^* \end{bmatrix}. \quad (30)$$

Relations between the equilibria and current sharing/voltage balancing are given in the next Proposition.

Proposition 7. *Consider system (27) with constant inputs \mathbf{I}_L^* and $\mathbf{V}_{\text{ref}}^*$. At the equilibrium, current sharing is achieved. Moreover, if $\mathbf{V}_{\text{ref}}^* = V_{\text{ref}} \mathbf{1}_N$ (i.e. if Assumption 1 holds) and α in (30) is equal to zero, then the equilibrium $[\Delta \mathbf{V}^{*T}, \mathbf{V}^{*T}]^T$ verifies the voltage balancing.*

Proof. Since equation (6) holds, one has that, at the equilibrium, relation (20) is verified. Then, the proof is identical to the one of Proposition 5. \square

Next, similarly to the simplified case described in Section 4.2.2, we evaluate the stability properties of the closed-loop system (27) so as to show the convergence of state $[\Delta \mathbf{V}^T \mathbf{V}^T]^T$ to an equilibrium which guarantees current sharing and voltage balancing.

4.3.2 Stability analysis

Proposition 8. *If $[\Delta \mathbf{V}^T \mathbf{V}^T]^T$ verifies (27), then*

$$\underbrace{\begin{bmatrix} \Delta \mathbf{V} \\ \mathbf{V} \end{bmatrix}}_{\mathbf{v}} = \underbrace{\begin{bmatrix} \overline{\Delta \mathbf{V}} \\ \overline{\mathbf{V}} \end{bmatrix}}_{\bar{\mathbf{v}}} + \underbrace{\begin{bmatrix} \widehat{\Delta \mathbf{V}} \\ \widehat{\mathbf{V}} \end{bmatrix}}_{\hat{\mathbf{v}}},$$

where $\bar{\mathbf{v}} \in H_{\perp}^1 \times H_{\perp}^1$ and $\hat{\mathbf{v}} \in H^1 \times H^1$ fulfill

$$\tilde{\Sigma}_{\perp}^1 : \begin{cases} \dot{\overline{\Delta \mathbf{V}}} = \mathbf{0}_N \\ \dot{\overline{\mathbf{V}}} = \Omega \overline{\Delta \mathbf{V}} - \Omega \overline{\mathbf{V}} + \Omega \overline{\mathbf{V}_{\text{ref}}} \end{cases} \quad (31a)$$

$$(31b)$$

and

$$\tilde{\Sigma}^1 : \begin{cases} \dot{\widehat{\Delta \mathbf{V}}} = -\mathbb{Q} \widehat{\mathbf{V}} - \mathbb{L} D \mathbf{I}_L \\ \dot{\widehat{\mathbf{V}}} = \Omega \widehat{\Delta \mathbf{V}} - \Omega \widehat{\mathbf{V}} + \Omega \widehat{\mathbf{V}_{\text{ref}}} \end{cases} \quad (32a)$$

$$(32b)$$

respectively.

Proof. The dynamics of $\overline{\Delta \mathbf{V}}$ and $\widehat{\Delta \mathbf{V}}$ can be derived proceeding as in the proof of Proposition 6. In a similar way, by averaging both sides of (27b), one derives the (independent) dynamics of $\overline{\mathbf{V}}$ and $\widehat{\mathbf{V}}$. \square

The above decomposition allows us to evaluate the evolution of state \mathbf{v} on $\mathbb{R}^{N \times N}$ by separately analyzing dynamics (31) and (32), i.e. studying the behavior of projections $\bar{\mathbf{v}} = P_{\mathcal{V}}(\mathbf{v})$ and $\hat{\mathbf{v}} = P_{\mathcal{W}}(\mathbf{v})$, with $\mathcal{V} = H_{\perp}^1 \times H_{\perp}^1$ and $\mathcal{W} = H^1 \times H^1$.

First we focus on $\tilde{\Sigma}_{\perp}^1$. Without loss of generality, for stability analysis we can neglect the input vector $\bar{\mathbf{V}}_{\text{ref}}$ in (31b), thus having:

$$\begin{cases} \dot{\bar{\mathbf{V}}} = \mathbf{0}_N \\ \dot{\bar{\mathbf{V}}} = \Omega \bar{\mathbf{D}} \bar{\mathbf{V}} - \Omega \bar{\mathbf{V}}. \end{cases} \quad (33a)$$

$$(33b)$$

By construction, (33b) collects the decoupled equations

$$\dot{\bar{V}}_i = \omega_c \bar{\Delta}V_i - \omega_c \bar{V}_i \quad \forall i = 1, \dots, N, \quad (34)$$

where, according to (31a), each term $\bar{\Delta}V_i$ in can be treated as an exogenous input (thus not affecting stability properties). It follows that dynamics (34) is asymptotically stable, since $\omega_c > 0$. In summary, system (31) tells us that the average $\bar{\Delta}\mathbf{V}$ will remain constant in time (and equal to $\langle \Delta\mathbf{V}_0 \rangle$), while $\bar{\mathbf{V}}$ will converge to the origin. For studying stability properties of system $\tilde{\Sigma}^1$, we consider (27) without inputs, i.e.

$$\begin{cases} \dot{\Delta}\mathbf{V} = -\mathbf{Q}\mathbf{V} \\ \dot{\mathbf{V}} = \Omega \Delta\mathbf{V} - \Omega \mathbf{V} \end{cases} \quad (35)$$

and analyze stability on $H^1 \times H^1$. We have the following result.

Theorem 2. *The origin of (35) is GES on $H^1 \times H^1$. Furthermore, matrix \mathbf{Q} has a simple zero eigenvalue and the rate of convergence is the maximum among real parts of all other eigenvalues.*

Proof. The proof is given in Appendix B. \square

By means of Theorem 2, we have that, given an initial condition $[\Delta\mathbf{V}_0^T \mathbf{V}_0^T]^T$ for system (27), the state $[\Delta\mathbf{V}^T \mathbf{V}^T]^T$ will converge to the equilibrium in (30), with $\alpha = \langle \Delta\mathbf{V}_0 \rangle$.

The results above show that, for system (27), current sharing is achieved in a GES fashion. In a similar way, asymptotic voltage balancing is ensured if Assumption 1 and (24) are fulfilled.

4.4 PnP design of secondary control

We now describe the procedure for designing secondary controllers in a PnP fashion. We will show that, as for the PnP design of primary regulators, when a DGU is added or removed, the secondary control layer can be updated only locally for preserving current sharing and voltage balancing. When a DGU (say DGU i) sends a plug-in request at a time \bar{t} , it chooses a set \mathcal{N}_i^c of communication neighbors and fixes parameters $a_{ij} > 0, \forall j \in \mathcal{N}_i^c$, in order to design the local consensus filter (5). At the same time, each DGU $j, j \in \mathcal{N}_i^c$, updates its consensus filter by setting $a_{ji} = a_{ij}$ in (5). Theorems 1 and 2 ensure that the disagreement dynamics of the mG states is GES, independently of \mathcal{N}_i^c . Let Assumption 1 hold for all the interconnected DGUs in the mG before \bar{t} and let us denote the common reference voltage by V_{ref} . If DGU i sets $V_{\text{ref},i} = V_{\text{ref}}$ and if we choose $\Delta V_i(\bar{t}) = 0$ (thus having $\langle \begin{bmatrix} \Delta\mathbf{V}'(\bar{t}) \\ \Delta V_i(\bar{t}) \end{bmatrix} \rangle = 0$, where $\Delta\mathbf{V}'(\bar{t})$ is the vector $\Delta\mathbf{V}$ prior the plugging-in of DGU i), both current sharing and voltage balancing are preserved in the asymptotic régime (see Propositions 5 and 7). Similarly, when a DGU (say DGU j) is unplugged at time \bar{t} , provided that the new graphs \mathcal{G}_{el} and \mathcal{G}_c fulfill Assumption 2, the key condition that must be guaranteed is that the vector $\Delta\mathbf{V}_{-j}$ (i.e. $\Delta\mathbf{V}$ without element j) verifies $\langle \Delta\mathbf{V}_{-j}(\bar{t}) \rangle = 0$. If $\langle \Delta\mathbf{V}(\bar{t}^-) \rangle = 0$, this can be achieved by re-setting

$$\Delta V_i(\bar{t}) = \Delta V_i(\bar{t}^-) + \frac{\Delta V_j(\bar{t}^-)}{|\mathcal{N}_j^c|}$$

for all $i \in \mathcal{N}_j^c$, and keeping $\Delta V_i(\bar{t}) = \Delta V_i(\bar{t}^-)$ for all $i \notin \mathcal{N}_j^c \cup \{j\}$. Indeed, this yields

$$\begin{aligned} \langle \Delta \mathbf{V}_{-\mathbf{j}}(\bar{t}) \rangle &= \frac{1}{N-1} \sum_{i \in \mathcal{N}_j^c} \Delta V_i(\bar{t}) + \frac{1}{N-1} \sum_{i \notin \mathcal{N}_j^c \cup \{j\}} \Delta V_i(\bar{t}) = \\ &= \frac{1}{N-1} \left(\sum_{i \in \mathcal{N}_j^c} \Delta V_i(\bar{t}^-) + \frac{1}{|\mathcal{N}_j^c|} \sum_{i \in \mathcal{N}_j^c} \Delta V_j(\bar{t}^-) + \sum_{i \notin \mathcal{N}_j^c \cup \{j\}} \Delta V_i(\bar{t}^-) \right) = \\ &= \frac{1}{N-1} (N \langle \Delta \mathbf{V}(\bar{t}^-) \rangle) = 0. \end{aligned}$$

5 Validation of secondary controllers

5.1 Simulation results

In this Section, we aim to demonstrate the capability of the proposed control scheme to guarantee current sharing and voltage balancing when DGUs are added or load changes occur. Simulations have been performed in Simulink/PLECS. We consider an mG composed of 5 DGUs, interconnected as in Figure 5, with non-identical electrical parameters and power lines. Notice that some DGUs have more than one neighbor, hence the impact of couplings on their dynamics will be larger. Moreover, the presence of a loop in the electrical network further complicates voltage regulation. Primary PnP voltage regulators are designed according to the method in [9], whereas, as regards the secondary control layer, we choose k_I in (6) equal to 0.2. DGUs have rated currents $I_{ti}^r = 10$ A, $i = 1, 2, 3$, $I_{t4}^r = 5$ A and $I_{t5}^r = 3.33$ A, and we aim to achieve current sharing proportional to them (i.e. all currents will have the same value when measured in p.u.). To this purpose, we set $I_{ti}^s = I_{ti}^r$, $i = 1, \dots, 5$. Furthermore, the voltage reference in Assumption 1 is $V_{ref} = 48$ V. All the electrical and control parameters are given in Appendix C.

Simulations have been performed assuming all-to-all communication among DGUs, with weights $a_{ij} > 0$. In the following, we describe Figure 6, which illustrates the evolution of the main electrical quantities (i.e. measured DGU output currents in Amperes, DGU output currents in p.u., PCC voltages and average PCCs voltage) during the consecutive simulation stages shown in Figure 5.

Stage 1: At time $t_0 = 0$, all the DGUs are assumed to be isolated and only the primary PnP voltage regulators, designed as in [9], are active. Therefore, as shown in Figure 6, (i) each DGU supplies its local load while keeping the corresponding PCC voltage at 48 V, and (ii) the DGU output currents in p.u. are different. We further highlight that primary controllers have been designed assuming that all the switches in Figure 5 connecting DGUs 1-4 are closed. From [9], however, they also stabilize the mG when all switches are open.

Stage 2: Subsystems 1-4 are connected together at time $t_1 = 5$ s and, according to the previous observation, no update of primary controllers is needed. At time t_1 we also activate the secondary control layer for DGUs 1-4, thus ensuring asymptotic current sharing among them (see the plot of the currents in p.u.). This is achieved by automatically adjusting the voltages at PCC (as shown in the plot of V_{PCC}). Moreover, the top plot of Figure 6 shows that, as expected, DGU 4 shares half of the current of DGUs 1-3. We further highlight that, by setting $\Delta V_i(t_1) = 0$, $i = 1, \dots, 4$, as described in Section 4.4, condition (24) is fulfilled and asymptotic voltage balancing is guaranteed (see the plot of V_{av}).

Stage 3: For evaluating the PnP capabilities of our control scheme, at $t_2 = 15$ s, DGU 5 sends a plug-in request to DGU 4. Previous primary controllers of DGUs 4 and 5 still fulfill the plug-in conditions in [9]: they are therefore maintained and the plug-in of DGU 5 is performed. At the same time, the secondary controller of DGU 5 is activated, and then the DGU contributes to current sharing. This can be noticed in Figure 6, as all PCC voltages change in order to let all the output currents in p.u. converge to a common value. At the same time, we notice that the measured output currents (top plot of Figure 6) are still shared accordingly (i.e. $I_{t1} = I_{t2} = I_{t3} = 2I_{t4} = 3I_{t5}$). Furthermore, choosing $\Delta V_5(t_2) = 0$ (as described in Section 4.4), we maintain the average PCCs voltage at 48 V (see V_{av} , stage 3).

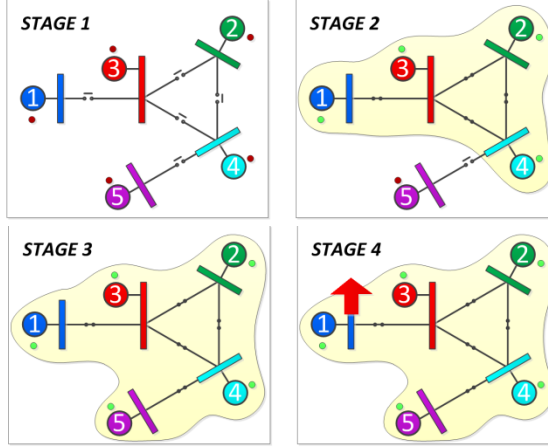


Figure 5: Simulation stages: numbered nodes represent DGUs and black lines denote power lines. The small circle next to each DGU is green if the secondary control layer is active for the corresponding unit, red otherwise. Open switches in stages 1 and 2 denote disconnected DGUs. The arrow in stage 4 represents a step up in the load current of DGU 1.

Stage 4: At $t_3 = 30$ s, we halve the load of DGU 1, thus increasing the corresponding load current I_{L1} and causing a peak in the corresponding output current. However, after few seconds, all the DGUs share again the total load current, while the averaged PCC voltage converges to the reference value.

5.2 Experimental results

Performance brought about by the presented hierarchical scheme been also validated via experimental tests based on the mG platform in the top-left panel of Figure 7, which consists of three *Danfoss* inverters, a dSPACE1103 control board and LEM sensors. In order to properly emulate DC/DC converters (i.e. Buck converters), only the first phase of each inverter has been used. Buck converters operate in parallel to emulate DGUs while different local load conditions have been obtained by connecting each PCC to a resistive load. All the converters are supplied by DC source generators. For this scenario, primary PnP voltage controllers are designed using the approach in [20], and we set k_I in (6) equal to 0.5. Moreover, we choose $I_{t1}^s = I_{t2}^s = I_{t3}^s = \bar{I}_t$, thus aiming to achieve the asymptotic current sharing condition (3). Overall, the controllers have been implemented in Simulink and compiled to the dSPACE system in order to command the Buck switches at a frequency of 10 kHz. Although the dSPACE platform is unique, separate local PnP voltage regulators have been implemented for each converter, so as to preserve the decentralized nature of the primary control layer.

We consider the mG in Figure 7, where \mathcal{G}_{el} and \mathcal{G}_c are highlighted in blue and red, respectively. The edges of \mathcal{G}_{el} are *RL* lines. In the sequel, we provide a detailed description of the evolution of the main electrical quantities, which are shown in Figure 8. At time $t_0 = 0$ s, all the DGUs are isolated and not connected to each other. At times $t_1 \approx 2.5$ s, $t_2 \approx 5$ s and $t_3 \approx 10$ s, we connect DGU 1 to 2, 2 to 3 and 1 to 3, respectively, thus obtaining a loop in the electrical topology. We recall that, since DGUs are equipped with PnP stabilizing regulators designed as in [20], no controller update is required when units are connected together. As shown in the plot of the PCC voltages in Figure 8, PnP primary voltage regulators ensure smooth transitions and stability. We also highlight that, since for $t < t_3$ the secondary layer is not active, the output currents are not equally shared and the PCC voltages coincide with the reference (notably, Assumption 1 holds, with $V_{ref} = 48$ V). Next, at time $t_4 \approx 15$ s, we set $\Delta V_i(t_4) = 0$, $i = 1, 2, 3$ and enable the secondary current layer. Since we choose the same scaling factor for all the DGUs, we have that the three output currents converge to the same measured value (see I_t in Figure 8). Furthermore,

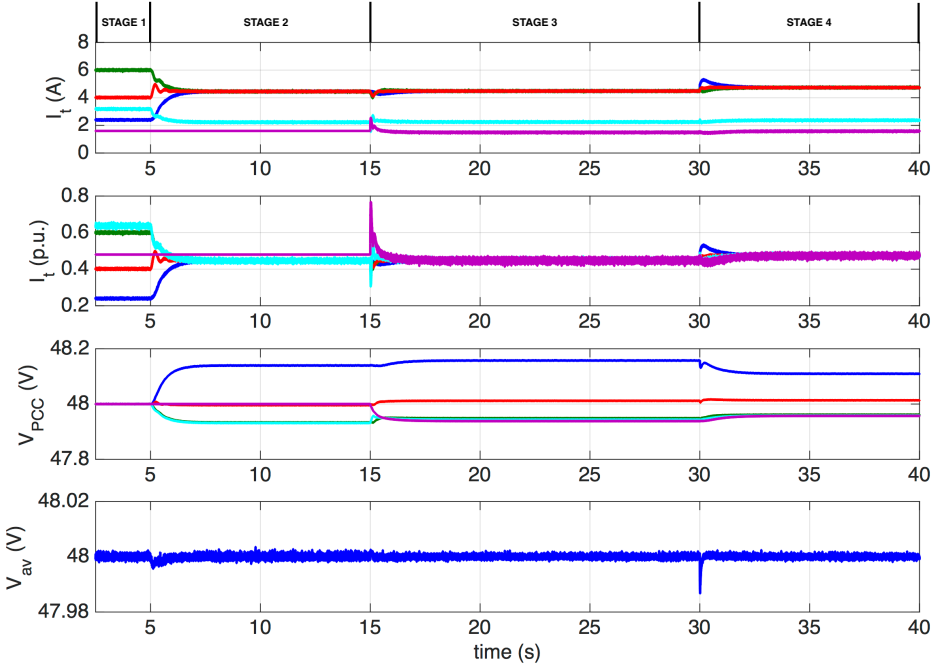


Figure 6: Simulation results: evolution of measured output currents, output currents in p.u., voltages at PCCs and average PCCs voltage. Lines in the plots are associated to different DGUs and they are color-coded as in Figure 5. Simulation stages are those shown in Figure 5.

similarly to the simulation example, the fulfillment of condition (24) guarantees asymptotic voltage balancing (see V_{av} in Figure 8). Finally, in order to assess the robustness of the proposed control scheme to unknown load dynamics, at time $t_5 \approx 25$ sec we decrease the load of DGU 3, causing an increment in the corresponding load current. As a consequence, the value of $\bar{I}_t = \langle \mathbf{I}_L^* \rangle$ increases as well. Also in this case, we have that the total load current is equally shared among DGUs while V_{av} do not deviate from 48 V.

6 Conclusions

In this paper, a secondary consensus-based control layer for current sharing and voltage balancing in DC mGs has been presented. Under the assumption that DGUs are equipped with decentralized primary controllers that guarantee voltage stability in the mG (e.g., PnP regulators), we proved stability of the hierarchical control scheme, current sharing and voltage balancing in the asymptotic régime. Moreover, we presented a method for designing secondary controllers in a PnP fashion for handling plugging -in/-out of DGUs. As regards future developments, communication delays [34, 35], will be included in the mathematical analysis. Furthermore, we will consider complex consensus controllers (e.g. proportional-integral regulators) for enhancing the convergence speed.

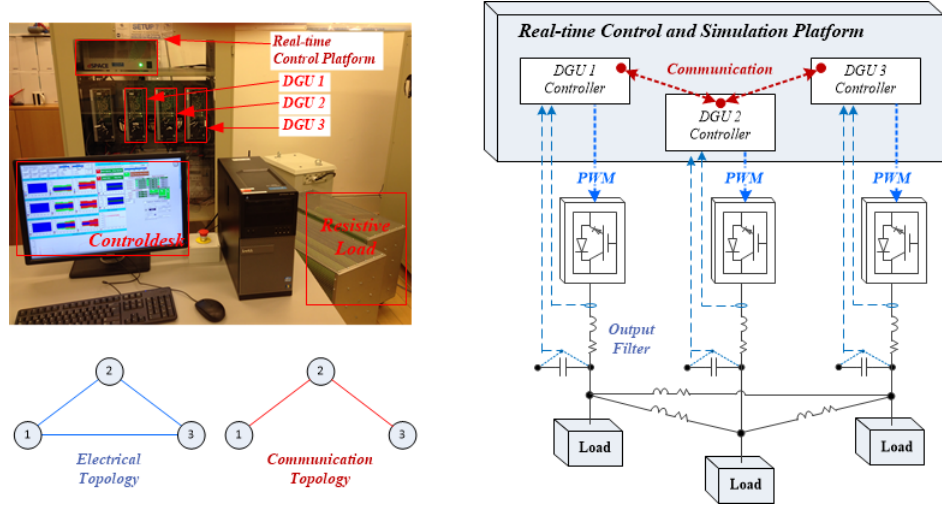


Figure 7: Experimental validation: mG setup (top-left), topologies of the electrical and communication graphs (bottom-left), and implemented control architecture (on the right).

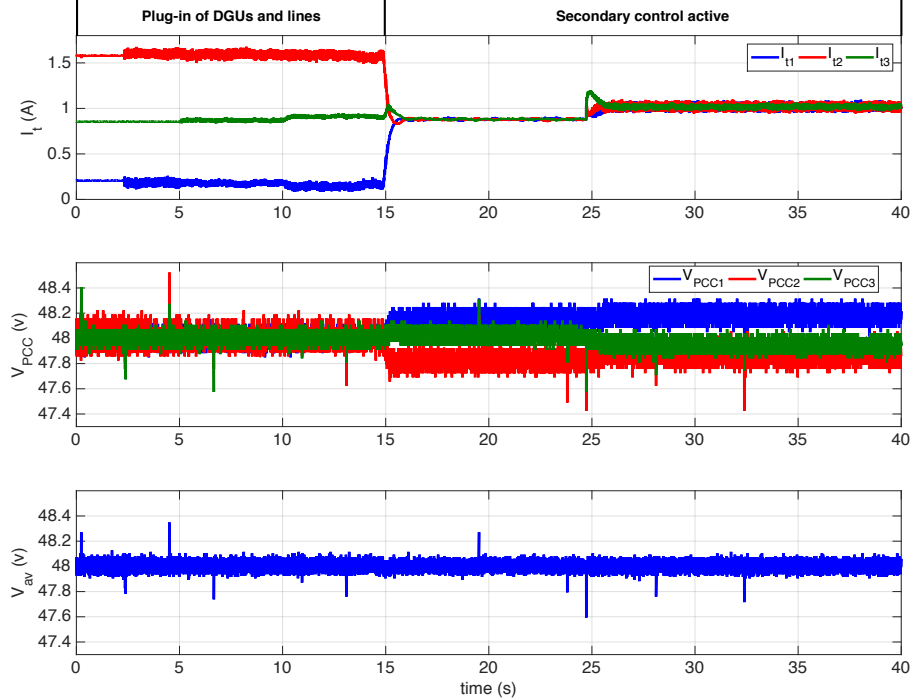


Figure 8: Experimental results for the mG in Figure 7. In the time interval from 2.5 s to 15 s, DGUs are connected together and primary PnP voltage regulators are enabled. From time 15 s onwards, also the secondary control layer is active. At time 25 s, the local load of DGU 3 is halved.

A Proof of Theorem 1

We introduce a preliminary Lemma, partly taken from Theorem 19 in [36].

Lemma 1. *For $\mathcal{A} \in \mathbb{R}^{n \times n}$, let \mathcal{V} and \mathcal{W} be \mathcal{A} -invariant subspaces of \mathbb{R}^n such that $\dim(\mathcal{V}) = k$, $\dim(\mathcal{W}) = n - k$ and $\mathbb{R}^n = \mathcal{V} \oplus \mathcal{W}$. Then:*

I) *there is a matrix $T \in \mathbb{R}^{n \times n}$ such that $A = T^{-1}\mathcal{A}T$ has the block-diagonal structure*

$$A = \begin{bmatrix} A_{11} & \mathbf{0} \\ \mathbf{0} & A_{22} \end{bmatrix}, \quad (36)$$

with $A_{11} \in \mathbb{R}^{k \times k}$ and $A_{22} \in \mathbb{R}^{(n-k) \times (n-k)}$. In particular, if $\{b_1, \dots, b_k\}$ and $\{b_{k+1}, \dots, b_n\}$ are basis for \mathcal{V} and \mathcal{W} , respectively, the transformation matrix T has the block structure

$$T = [b_1 | \dots | b_k | b_{k+1} | \dots | b_n]. \quad (37)$$

Therefore, if $x \in \mathcal{V}$, then $T^{-1}x = \begin{bmatrix} \tilde{x}_1 \\ 0 \end{bmatrix}$ with $\tilde{x}_1 \in \mathbb{R}^k$. Similarly, if $x \in \mathcal{W}$, then $T^{-1}x = \begin{bmatrix} 0 \\ \tilde{x}_2 \end{bmatrix}$ with $\tilde{x}_2 \in \mathbb{R}^{n-k}$.

II) *The origin of $\dot{x} = \mathcal{A}x$ is GES on \mathcal{V} if and only if the origin of $\dot{\tilde{x}}_1 = A_{11}\tilde{x}_1$ is GES. Moreover, parameters $\kappa, \eta > 0$ verifying $\|\tilde{x}_1(t)\| \leq \kappa e^{-\eta t} \|\tilde{x}_1(0)\|$, also guarantee $\|P_{\mathcal{V}}x(t)\| \leq \kappa e^{-\eta t} \|P_{\mathcal{V}}x(0)\|$.*

Proof. For the proof of point I, we defer the reader to the proof of Theorem 19 in [36].

The proof of point II directly follows from the block-diagonal structure of matrix A in (36). Indeed,

$$\dot{x} = \mathcal{A}x \Leftrightarrow \dot{\tilde{x}} = A \begin{bmatrix} \tilde{x}_1 \\ \tilde{x}_2 \end{bmatrix} \Leftrightarrow \begin{cases} \dot{\tilde{x}}_1 = A_{11}\tilde{x}_1 \\ \dot{\tilde{x}}_2 = A_{22}\tilde{x}_2, \end{cases}$$

i.e. A_{11} is the matrix representation of the map $\mathcal{A}(\mathcal{V}|\mathcal{V})$. In other words, studying the stability of \mathcal{A} on \mathcal{V} is equivalent to study the stability of A_{11} . Moreover, by construction, $P_{\mathcal{V}}(x) = T \begin{bmatrix} \tilde{x}_1 \\ 0 \end{bmatrix}$. Then,

$$\|P_{\mathcal{V}}(x(t))\| \leq \|T\| \|\tilde{x}_1(t)\| \leq \|T\| \kappa e^{-\eta t} \|\tilde{x}_1(0)\|. \quad (38)$$

Since $\|\tilde{x}_1(0)\| \leq \|T^{-1}\| \|P_{\mathcal{V}}(x(0))\|$, inequality (38) becomes

$$\|P_{\mathcal{V}}(x)\| \leq \|T\| \kappa e^{-\eta t} \|\tilde{x}_1(0)\| \leq \kappa e^{-\eta t} \|P_{\mathcal{V}}(x(0))\|.$$

□

Proof of Theorem 1. Points (i) and (ii) of Proposition 3 show that subspaces H^1 and H_{\perp}^1 are \mathbb{Q} -invariant. Moreover, $\mathbb{R}^N = H^1 \oplus H_{\perp}^1$. It follows that Lemma 1 can be applied with $\mathcal{V} = H^1$ and $\mathcal{W} = H_{\perp}^1$. In particular, by means of point I, we know that there exists a transformation matrix $T \in \mathbb{R}^{N \times N}$ such that the linear map \mathbb{Q} can be represented as in (36). Denoting with $B^1 = \{b_1, \dots, b_{N-1}\}$ and $B_{\perp}^1 = \mathbf{1}_N$ the basis for H^1 and H_{\perp}^1 , respectively, from (37), we have

$$T = [b_1 | \dots | b_{N-1} | \mathbf{1}_N].$$

Matrix $Q = T^{-1}\mathbb{Q}T$ is given by

$$Q = \begin{bmatrix} Q_{11} & \mathbf{0} \\ \mathbf{0} & q_{22} \end{bmatrix} \quad (39)$$

where $Q_{11} \in \mathbb{R}^{(N-1) \times (N-1)}$. Moreover, scalar $q_{22} = 0$ since, by construction, it represents the map $\mathbb{Q}(H_{\perp}^1|H_{\perp}^1)$ (see Proposition 3-(i)). We notice that the representations of $\widehat{\Delta \mathbf{V}}$ and $\overline{\Delta \mathbf{V}}$ with

respect to the basis \mathcal{B} are $\tilde{v}_1 = T^{-1}\widehat{\Delta\mathbf{V}} = [\xi_1, \dots, \xi_{N-1}, 0]^T$ and $\tilde{v}_\perp = T^{-1}\overline{\Delta\mathbf{V}} = [0, \dots, 0, \xi_N]^T$, respectively. Now we prove that the origin of

$$\dot{\tilde{v}}_1 = -Q_{11}\tilde{v}_1 \quad (40)$$

is GES. Since Q and \mathbb{Q} are similar matrices, they have the same eigenvalues. Therefore, by exploiting points (iv) and (v) of Proposition 3, one has that all the eigenvalues of Q_{11} are strictly positive. This proves that (40) is GES and, as shown in [36], the convergence rate is $-\lambda$, where λ is the minimal eigenvalue of Q_{11} . The remainder of the proof follows directly from point II of Lemma 1. \square

B Proof of Theorem 2

We first present two Propositions which provide preliminary results that will be used to prove Theorem 2.

Proposition 9. *Subspaces $H^1 \times H^1$ and $H_\perp^1 \times H_\perp^1$ are \mathcal{Q} -invariant.*

Proof. We first show that, for any vector $\hat{\mathbf{v}} = [\hat{\mathbf{v}}_1^T \hat{\mathbf{v}}_2^T]^T$, it holds $\mathcal{Q}\hat{\mathbf{v}} \in H^1 \times H^1$. Indeed,

$$\mathcal{Q}\hat{\mathbf{v}} = \begin{bmatrix} \mathbf{0}_N & -\mathbb{Q} \\ \Omega & -\Omega \end{bmatrix} \begin{bmatrix} \hat{\mathbf{v}}_1 \\ \hat{\mathbf{v}}_2 \end{bmatrix} = \begin{bmatrix} -\mathbb{Q}\hat{\mathbf{v}}_2 \\ \Omega(\hat{\mathbf{v}}_1 - \hat{\mathbf{v}}_2) \end{bmatrix},$$

and, from Proposition 3-(iii), the rightmost vector belongs to $H^1 \times H^1$. Similarly, for any vector $\bar{\mathbf{v}} = [\bar{\mathbf{v}}_1^T \bar{\mathbf{v}}_2^T]^T \in H_\perp^1 \times H_\perp^1$, we have that

$$\mathcal{Q}\bar{\mathbf{v}} = \begin{bmatrix} \mathbf{0}_N & -\mathbb{Q} \\ \Omega & -\Omega \end{bmatrix} \begin{bmatrix} \bar{\mathbf{v}}_1 \\ \bar{\mathbf{v}}_2 \end{bmatrix} = \begin{bmatrix} \mathbf{0}_N \\ \Omega(\bar{\mathbf{v}}_1 - \bar{\mathbf{v}}_2) \end{bmatrix}$$

and then $\mathcal{Q}\bar{\mathbf{v}} \in H_\perp^1 \times H_\perp^1$. \square

Proposition 10. *Matrix \mathcal{Q} has two eigenvalues equal to zero and $-\omega_c$, respectively. All other eigenvalues have strictly negative real part.*

Proof. By definition, vector $[\Delta\mathbf{V}^T \mathbf{V}^T]^T \neq \mathbf{0}_{2N}$ is an eigenvector of \mathcal{Q} , if there exists λ_i such that

$$\begin{bmatrix} \mathbf{0} & -\mathbb{Q} \\ \Omega & -\Omega \end{bmatrix} \begin{bmatrix} \Delta\mathbf{V} \\ \mathbf{V} \end{bmatrix} = \lambda_i \begin{bmatrix} \Delta\mathbf{V} \\ \mathbf{V} \end{bmatrix}. \quad (41)$$

From (41), one gets:

$$-\mathbb{Q}\mathbf{V} = \lambda_i \Delta\mathbf{V} \quad (42a)$$

$$\omega_c(\Delta\mathbf{V} - \mathbf{V}) = \lambda_i \mathbf{V}. \quad (42b)$$

By isolating $\Delta\mathbf{V}$ in (42b) and substituting it in (42a), we obtain

$$-\mathbb{Q}\mathbf{V} = \underbrace{\frac{\lambda_i(\lambda_i + \omega_c)}{\omega_c}}_{\hat{\lambda}_i} \mathbf{V}. \quad (43)$$

where $\hat{\lambda}_i$ are, by construction, eigenvalues of $-\mathbb{Q}$. From points (iv) and (v) of Proposition 3, we have

$$\hat{\lambda}_N = 0 \quad (44a)$$

$$\hat{\lambda}_i = -\gamma_i, \quad \gamma_i > 0 \quad i = 1, \dots, N-1. \quad (44b)$$

From (44a) and (43), one has

$$\lambda_i(\lambda_i + \omega_c) = 0$$

and hence \mathcal{Q} has a single eigenvalue equal to zero and an eigenvalue equal to $-\omega_c$. By substituting in (44b) the expression of $\hat{\lambda}_i$ in (43), one gets:

$$\frac{\lambda_i^2}{\omega_c} + \lambda_i + \gamma_i = 0 \quad i = 1, \dots, N-1. \quad (45)$$

Since all the coefficients of the polynomial in (45) are strictly positive, we can conclude that matrix \mathcal{Q} has $2(N-1)$ eigenvalues with $\text{Re}(\lambda_i) < 0$. \square

Proof of Theorem 2. Similarly to the proof of Theorem 1, we can exploit Lemma 1 with $\mathcal{V} = H^1 \times H^1$ and $\mathcal{W} = H_\perp^1 \times H_\perp^1$. In fact, we know that (i) subspaces $H^1 \times H^1$ and $H_\perp^1 \times H_\perp^1$ are \mathcal{Q} -invariant (see Proposition 9) and (ii) $\mathbb{R}^N \times \mathbb{R}^N = \mathcal{V} \oplus \mathcal{W}$. Hence, there exists a transformation matrix $T \in \mathbb{R}^{2N \times 2N}$ such that the linear map \mathcal{Q} has an equivalent block-diagonal representation of the form (36), i.e.

$$T^{-1} \mathcal{Q} T = Q = \left[\begin{array}{c|c} Q_{11} & \mathbf{0} \\ \hline \mathbf{0} & Q_{22} \end{array} \right], \quad (46)$$

with $Q_{11} \in \mathbb{R}^{2(N-1) \times 2(N-1)}$ and $Q_{22} \in \mathbb{R}^{2 \times 2}$. By construction, matrices Q_{11} and Q_{22} in (46) represent the maps $\mathcal{Q}(\mathcal{V}|\mathcal{V})$ and $\mathcal{Q}(\mathcal{W}|\mathcal{W})$, respectively. In particular, in the light on the consideration made for system (31), we have that the eigenvalues of Q_{22} are zero and $-\omega_c$. Moreover, by construction, the eigenvalues of Q_{11} are the $2(N-1)$ eigenvalues of \mathcal{Q} with strictly negative real part (see Proposition 10). \square

C Electrical and simulation parameters

In this appendix, we provide the electrical and control parameters of the simulation scenario described in Section 5.1.

Table 1: Electrical setup and line parameters

| Converter and output filter parameters | | | |
|--|--------------------------|-----------------------|----------------------|
| Input/Output DC voltage (V) | | | 100/48 |
| DGU | Resistance $R_t(\Omega)$ | Capacitance $C_t(mF)$ | Inductance $L_t(mH)$ |
| $\hat{\Sigma}_{[1]}^{DGU}$ | 0.2 | 2.2 | 1.8 |
| $\hat{\Sigma}_{[2]}^{DGU}$ | 0.3 | 1.9 | 2.0 |
| $\hat{\Sigma}_{[3]}^{DGU}$ | 0.1 | 1.7 | 2.2 |
| $\hat{\Sigma}_{[4]}^{DGU}$ | 0.5 | 2.5 | 3.0 |
| $\hat{\Sigma}_{[5]}^{DGU}$ | 0.4 | 2.0 | 1.3 |

| Tie lines parameters | | |
|-------------------------|--------------------------|-------------------------|
| Connected DGUs (i, j) | Resistance $R_s(\Omega)$ | Inductance $L_s(\mu H)$ |
| (1, 3) | 0.07 | 2.1 |
| (2, 3) | 0.04 | 2.3 |
| (2, 4) | 0.08 | 1.8 |
| (3, 4) | 0.07 | 1 |
| (4, 5) | 0.05 | 2 |

Table 2: Primary and secondary control layer parameters.

| Primary PnP control layer | |
|---------------------------|-------------------------------|
| K_1 | $[-2.134 \ -0.163 \ 13.553]$ |
| K_2 | $[-0.869 \ -0.050 \ 48.285]$ |
| K_3 | $[-0.480 \ -0.108 \ 30.673]$ |
| K_4 | $[-6.990 \ -0.175 \ 102.960]$ |
| K_5 | $[-0.101 \ -0.010 \ 16.393]$ |

| Secondary consensus layer | |
|---------------------------|-----|
| k_I | 0.2 |

References

- [1] A. Ipakchi and F. Albuyeh, "Grid of the future," *Power and Energy Magazine, IEEE*, vol. 7, no. 2, pp. 52–62, 2009.
- [2] J. M. Guerrero, M. Chandorkar, T. L. Lee, and P. C. Loh, "Advanced control architectures for intelligent microgrids - part I: decentralized and hierarchical control," *IEEE Transactions on Industrial Electronics*, vol. 60, no. 4, pp. 1254–1262, 2013.
- [3] S. Riverso, F. Sarzo, and G. Ferrari-Trecate, "Plug-and-play voltage and frequency control of islanded microgrids with meshed topology," *IEEE Transactions on Smart Grid*, vol. 6, no. 3, pp. 1176–1184, 2015.
- [4] S. Bolognani and S. Zampieri, "A distributed control strategy for reactive power compensation in smart microgrids," *IEEE Transactions on Automatic Control*, vol. 58, no. 11, pp. 2818–2833, 2013.
- [5] J. Schiffer, T. Seel, J. Raisch, and T. Sezi, "Voltage stability and reactive power sharing in inverter-based microgrids with consensus-based distributed voltage control," *IEEE Transactions on Control Systems Technology*, vol. 24, no. 1, pp. 96–109, 2016.
- [6] J. W. Simpson-Porco, F. Dörfler, and F. Bullo, "Voltage stabilization in microgrids via quadratic droop control," *IEEE Transactions on Automatic Control*, vol. PP, no. 99, pp. 1–1, 2016.
- [7] T. Dragicevic, X. Lu, J. C. Vasquez, and J. M. Guerrero, "DC microgrids-part I: A review of control strategies and stabilization techniques," *IEEE Transactions on Power Electronics*, vol. 31, no. 7, pp. 4876–4891, 2016.
- [8] A. T. Elsayed, A. A. Mohamed, and O. A. Mohammed, "DC microgrids and distribution systems: An overview," *Electric Power Systems Research*, vol. 119, pp. 407–417, 2015.
- [9] M. Tucci, S. Riverso, J. C. Vasquez, J. M. Guerrero, and G. Ferrari-Trecate, "A decentralized scalable approach to voltage control of DC islanded microgrids," *IEEE Transactions on Control Systems Technology*, vol. 24, no. 6, pp. 1965–1979, 2016.
- [10] J. Zhao and F. Dörfler, "Distributed control and optimization in DC microgrids," *Automatica*, vol. 61, pp. 18–26, 2015.
- [11] C. De Persis, E. Weitenberg, and F. Dörfler, "A power consensus algorithm for DC microgrids," *arXiv preprint arXiv:1611.04192*, 2016.
- [12] G. Cezar, R. Rajagopal, and B. Zhang, "Stability of interconnected DC converters," in *54th Conference on Decision and Control*, 2015, pp. 9–14.
- [13] M. Hamzeh, M. Ghafouri, H. Karimi, K. Sheshyekani, and J. M. Guerrero, "Power oscillations damping in DC microgrids," *IEEE Transactions on Energy Conversion*, vol. 31, no. 3, pp. 970–980, 2016.
- [14] D. Zonetti, R. Ortega, and A. Benchaib, "A globally asymptotically stable decentralized PI controller for multi-terminal high-voltage DC transmission systems," in *13th European Control Conference*, 2014, pp. 1397–1403.
- [15] H. Han, X. Hou, J. Yang, J. Wu, M. Su, and J. M. Guerrero, "Review of power sharing control strategies for islanding operation of ac microgrids," *IEEE Transactions on Smart Grid*, vol. 7, no. 1, pp. 200–215, 2016.
- [16] Q. Shafiee, T. Dragicevic, F. Andrade, J. C. Vasquez, and J. M. Guerrero, "Distributed consensus-based control of multiple DC-microgrids clusters," in *Industrial Electronics Society, IECON 2014-40th Annual Conference of the IEEE*, 2014, pp. 2056–2062.

- [17] L. Meng, T. Dragicevic, J. Roldán-Pérez, J. C. Vasquez, and J. M. Guerrero, “Modeling and sensitivity study of consensus algorithm-based distributed hierarchical control for DC microgrids,” *IEEE Transactions on Smart Grid*, vol. 7, no. 3, pp. 1504–1515, 2016.
- [18] M. Andreasson, D. V. Dimarogonas, H. Sandberg, and K. H. Johansson, “Control of MTDC transmission systems under local information,” in *53rd Conference on Decision and Control*, 2014, pp. 1335–1340.
- [19] H. Behjati, A. Davoudi, and F. Lewis, “Modular DC-DC converters on graphs: cooperative control,” *IEEE Transactions on Power Electronics*, vol. 29, no. 12, pp. 6725–6741, 2014.
- [20] M. Tucci, S. Riverso, and G. Ferrari-Trecate, “Voltage stabilization in DC microgrids through coupling-independent plug-and-play controllers,” in *55th Conference on Decision and Control*, 2016, pp. 4944–4949.
- [21] A. Jadbabaie, J. Lin, and A. S. Morse, “Coordination of groups of mobile autonomous agents using nearest neighbor rules,” *IEEE Transactions on Automatic Control*, vol. 48, no. 6, pp. 988–1001, 2003.
- [22] J. Allmeling and W. Hammer, “PLECS-User Manual,” 2013.
- [23] F. Bullo, *Lectures on Network Systems*. Version 0.85, 2016, <http://motion.me.ucsb.edu/book-lns>.
- [24] R. Grone, R. Merris, and V. S. Sunder, “The Laplacian spectrum of a graph,” *SIAM Journal on Matrix Analysis and Applications*, vol. 11, no. 2, pp. 218–238, 1990.
- [25] A. Bensoussan and J. L. Menaldi, “Difference equations on weighted graphs,” *Journal of Convex Analysis*, vol. 12, no. 1, pp. 13–44, 2005.
- [26] G. Ferrari-Trecate, A. Buffa, and M. Gati, “Analysis of coordination in multi-agent systems through partial difference equations,” *IEEE Transactions on Automatic Control*, vol. 51, no. 6, pp. 1058–1063, June 2006.
- [27] Y. Hong and R. A. Horn, “The Jordan canonical form of a product of a hermitian and a positive semidefinite matrix,” *Linear Algebra and Its Applications*, vol. 147, pp. 373–386, 1991.
- [28] R. Agaev and P. Chebotarev, “On the spectra of nonsymmetric laplacian matrices,” *Linear Algebra and its Applications*, vol. 399, pp. 157–168, 2005.
- [29] C. Godsil and G. Royle, “Algebraic graph theory, volume 207 of Graduate Texts in Mathematics,” 2001.
- [30] S. Lang, “Linear algebra. Undergraduate texts in mathematics,” Springer-Verlag, 1987.
- [31] R. Olfati-Saber and R. M. Murray, “Consensus problems in networks of agents with switching topology and time-delays,” *IEEE Transactions on Automatic Control*, vol. 49, no. 9, pp. 1520–1533, 2004.
- [32] M. C. Pease, *Methods of matrix algebra*. Academic Press New York, 1965.
- [33] R. A. Horn and C. R. Johnson, *Matrix analysis*. Cambridge university press, 2012.
- [34] P. A. Bliman and G. Ferrari-Trecate, “Average consensus problems in networks of agents with delayed communications,” *Automatica*, vol. 44, no. 8, pp. 1985–1995, 2008.
- [35] L. Meng, T. Dragicevic, J. M. Guerrero, and J. C. Vasquez, “Dynamic consensus algorithm based distributed global efficiency optimization of a droop controlled DC microgrid,” in *Energy Conference (ENERGYCON), 2014 IEEE International*, 2014, pp. 1276–1283.
- [36] F. M. Callier and C. A. Desoer, *Linear system theory*. Springer Science & Business Media, 2012.